Develop Particle-Orbit-Tracking Model for Tokamak Burning Plasmas

Zheng-Xiong Wang and PTC Team

Dalian University of Technology, Dalian, China

Outline

1. Background
2. PTC Model: Fundamentals
3. Applications
4. Summary

Outline

Background

Fast particles play a crucial role in burning plasmas.

- provide heating
- provide current drive
- trigger instabilities

Gyro-kinetic / Full-kinetic simulation for Tokamak plasmas

- Self-consistent turbulence and transport simulation
- $>10^6$ particles, ~1M CPU hours for nonlinear global EM simulation
- **Difficult to carry out long-time-scale simulations of macroscopic parameters**

Test particle orbit-tracking simulations

✓ **Low computational cost**

Only need to track orbits without solving for the self-consistent field evolution.

✓ **Great flexibility**

Easily adaptable to different magnetic configurations and external heating/driving schemes.

✓ **Close connection with experiments**

Commonly used to interpret fast ion diagnostic signals and impurity transport phenomena.

Outline

Particle Orbit for Fast Ions and Runaway Electrons

- Multiple orbit types： full, drift orbit, relativistic orbit with collisions
- Modeling of NBI for heating, current drive, ICRF, and fueling
- Modeling of alpha particle confinement & heating
- Modeling of runaway electron dynamics
- ……

Orbits for Fast Ions

Guiding center orbit:

$$\frac{d\mathbf{X}}{dt} = \frac{\mathbf{B}^*}{B_\parallel^*} v_\parallel + \frac{\mu}{m\Omega B_\parallel^*} \mathbf{B} \times \nabla B + \frac{1}{BB_\parallel^*} \mathbf{E} \times \mathbf{B}$$

$$\frac{dv_\parallel}{dt} = -\frac{\mu}{m} \frac{\mathbf{B}^*}{B_\parallel^*} \cdot \nabla B + \frac{Ze}{m} \frac{\mathbf{B}^*}{B_\parallel^*} \cdot \mathbf{E}$$

$$\mathbf{B}^\star = \mathbf{B} + B\frac{v_\parallel}{\Omega} \nabla \times \mathbf{b}$$

$$B_\parallel^\star \equiv \mathbf{b} \cdot \mathbf{B}^\star = B\left(1 + \frac{v_\parallel}{\Omega} \mathbf{b} \cdot \nabla \times \mathbf{b},\right)$$

$$\mathbf{b} = \mathbf{B}/B, \Omega = \frac{qB}{m}$$

Full orbit:

$$\frac{d\mathbf{v}}{dt} = \frac{q}{m}(\mathbf{v} \times \mathbf{B} + \mathbf{E}) + \dot{\mathbf{v}}_c$$

$$\frac{d\mathbf{x}}{dt} = \mathbf{v},$$

Orbit for Runaway Electrons

Guiding center orbit:

$$\dot{\mathbf{X}} = \{\mathbf{X}, H\}_{\mathrm{gc}} = \frac{p_\parallel^\star}{\gamma_r m_0} \frac{\mathbf{B}^*}{B_\parallel^*} + \frac{\mathbf{b}^*}{qB_\parallel^*} \times \left(\nabla H + \frac{\partial \mathbf{A}^*}{\partial t}\right),$$

$$\dot{p_\parallel} = \{p_\parallel, H\}_{\mathrm{gc}} = -\frac{\mathbf{B}^*}{B_\parallel^*} \cdot \left(\nabla H + \frac{\partial \mathbf{A}^*}{\partial t}\right),$$

$$\dot{\mu} = \{\mu, H\}_{\mathrm{gc}} = 0,$$

$$\dot{\theta} = \{\theta, H\}_{\mathrm{gc}} = \frac{qB}{\gamma_r m_0},$$

Full orbit：

$$\frac{d\mathbf{x}}{dt} = \mathbf{v} \qquad \gamma = \frac{1}{\sqrt{1 - (v/c)^2}}$$

$$\frac{d\mathbf{p}}{dt} = -e(\mathbf{E} + \mathbf{v} \times \mathbf{B}) + \mathbf{F}_R \qquad \mathbf{F}_R = -P_R \frac{\mathbf{v}}{v^2}$$

$$\mathbf{p} = \gamma m_e \mathbf{v}$$

$$P_R = \frac{e^2}{6\pi\epsilon_0 c} \gamma^6 \left[\left|\frac{\mathbf{a}}{c}\right|^2 - \left|\frac{\mathbf{v} \times \mathbf{a}}{c}\right|^2\right]$$

Coulomb collisions: Fokker-Planck equation

$$\frac{\partial f_\alpha(\mathbf{v}, t)}{\partial t} = \left[-\frac{\partial}{\partial v_i} F_i(\mathbf{v}, t) + \frac{1}{2} \frac{\partial^2}{\partial \mathrm{v}_i \partial \mathrm{v}_k} D_{ik}(\mathbf{v}, t)\right] f_\alpha(\mathbf{v}, t)$$

$$\frac{d\mathrm{v}_i}{dt} = F_i(\mathrm{v}, t) + \sqrt{D_{ii}(\mathrm{v}, t)}\xi_i(t).$$

$$\Delta \mathrm{v}_\parallel = -\nu_{sd} \Delta t_{ec} \mathrm{v}_0 + \sqrt{\nu_\parallel \Delta t_{ec} \mathrm{v}_0 N_1}$$

$$\Delta \mathrm{v}_{\perp 1,2} = \sqrt{\frac{\nu_\perp \Delta t_{ec}}{2}} \mathrm{v}_0 N_{2,3}$$

$$\mathbf{v} = \mathbf{v}_0 + \Delta \mathrm{v}_\parallel \hat{e}_1 + \Delta \mathrm{v}_{\perp 1} \hat{e}_2 + \Delta \mathrm{v}_{\perp 2} \hat{e}_3.$$

Fokker-Planck equation based on quasi-linear theory

$$\frac{\partial}{\partial t} f_0(\boldsymbol{v}, t) = -\frac{\partial}{\partial \boldsymbol{v}} (\boldsymbol{\Gamma} f_0) + \frac{1}{2} \frac{\partial}{\partial \boldsymbol{v}} \frac{\partial}{\partial \boldsymbol{v}} : (2\mathbb{D} f_0)$$

$$D_{\perp\perp} = \boldsymbol{e}_\perp \cdot \mathbb{D} \cdot \boldsymbol{e}_\perp = \sum_n \frac{\pi}{2} \frac{q^2}{m^2} \delta(\omega - k_\parallel v_\parallel - n\omega_c) \left(\frac{n\omega_c}{\omega}\right)^2 s_n^2$$

$$D_{\parallel\parallel} = \boldsymbol{e}_\parallel \cdot \mathbb{D} \cdot \boldsymbol{e}_\parallel = \sum_n \frac{\pi}{2} \frac{q^2}{m^2} \delta(\omega - k_\parallel v_\parallel - n\omega_c) \left(\frac{k_\parallel v_\perp}{\omega}\right)^2 s_n^2$$

$$D_{\perp\parallel} = D_{\parallel\perp} = \sqrt{D_{\perp\perp} D_{\parallel\parallel}}$$

$$s_n = \frac{E_+}{\sqrt{2}} J_{n-1}(\alpha) + \frac{E_-}{\sqrt{2}} J_{n+1}(\alpha) + \left(\frac{v_\parallel}{v_\perp}\right) E_\parallel J_n(\alpha)$$

The Program Flowchart of PTC

Program flowchart

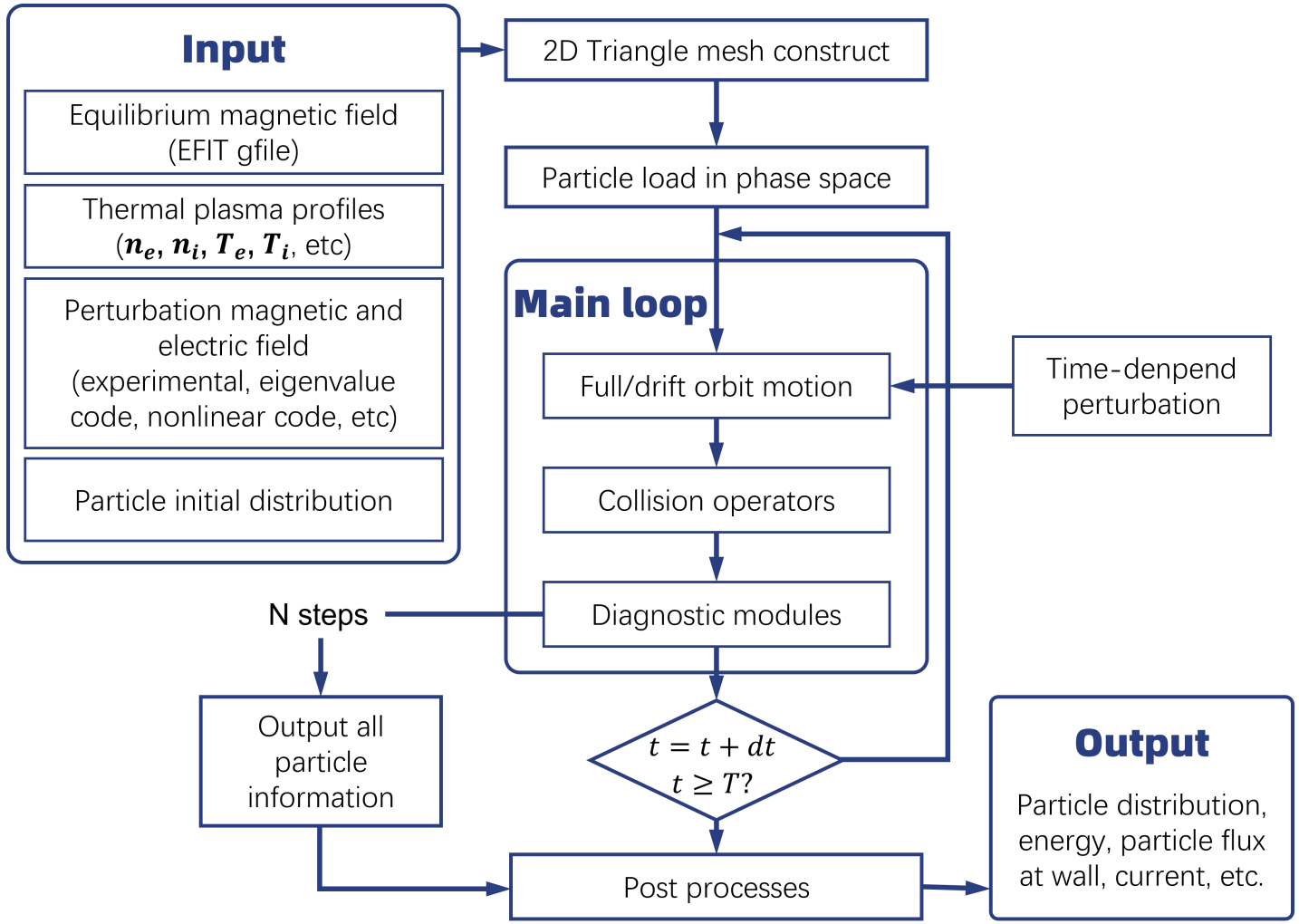

Applications

- Alpha particles source
- Alpha particles slowing down distribution in 2D equilibrium
- Energetic particles current drive
- Torque induced by energetic particles
- Fast ions transport and loss in 3D perturbation: TF Ripple, MHD instabilities, Alfven instabilities, Multiple mode together
- Runaway electron modeling
- ……

Transport of Alpha Particles in CFETR

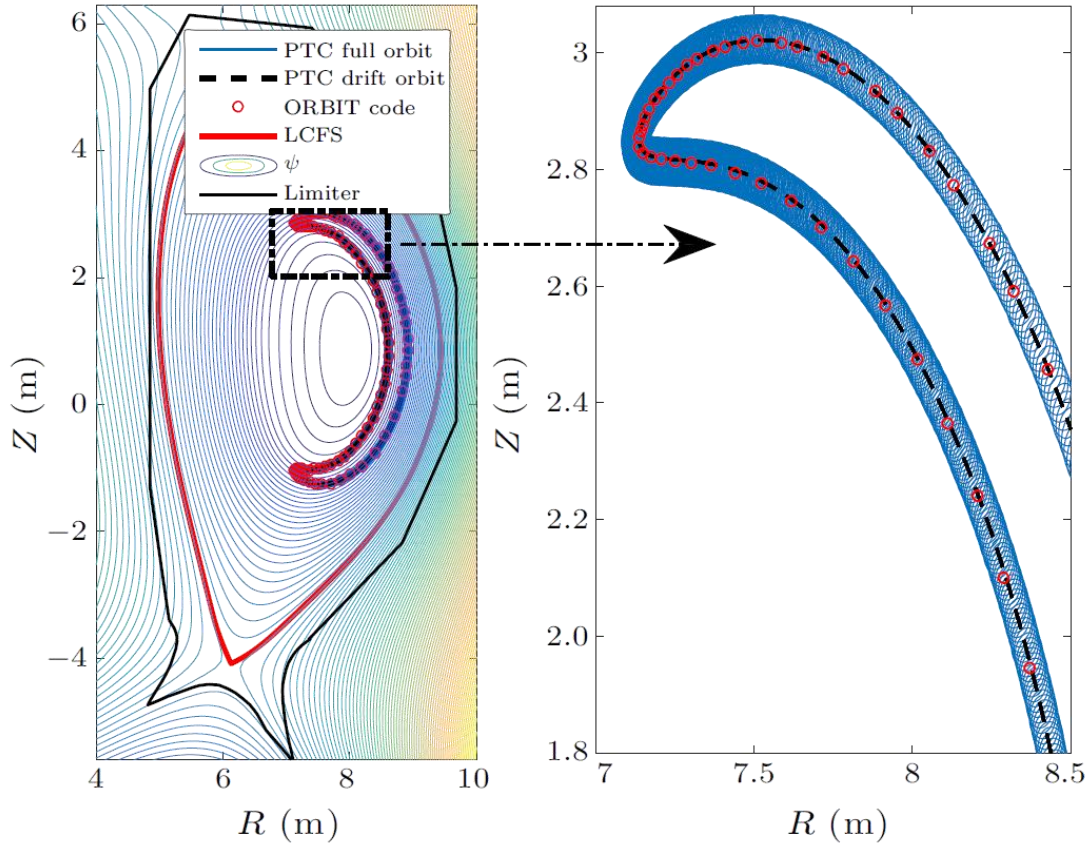

Orbit comparison for an α particle in the CFETR 2019 steady-state scenario.

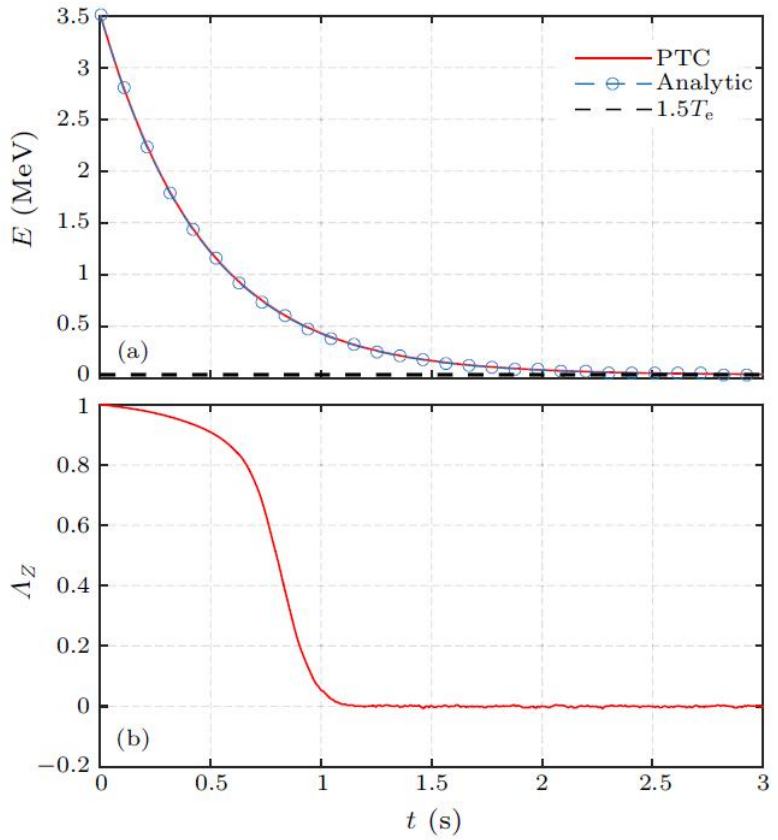

Evolution of (a) α particle slowing down test, (b) pitch angle scattering test.

- PTC has completed benchmark for **α particle** trajectories and slowing-down calculation

Transport of Runaway Electrons in ITER

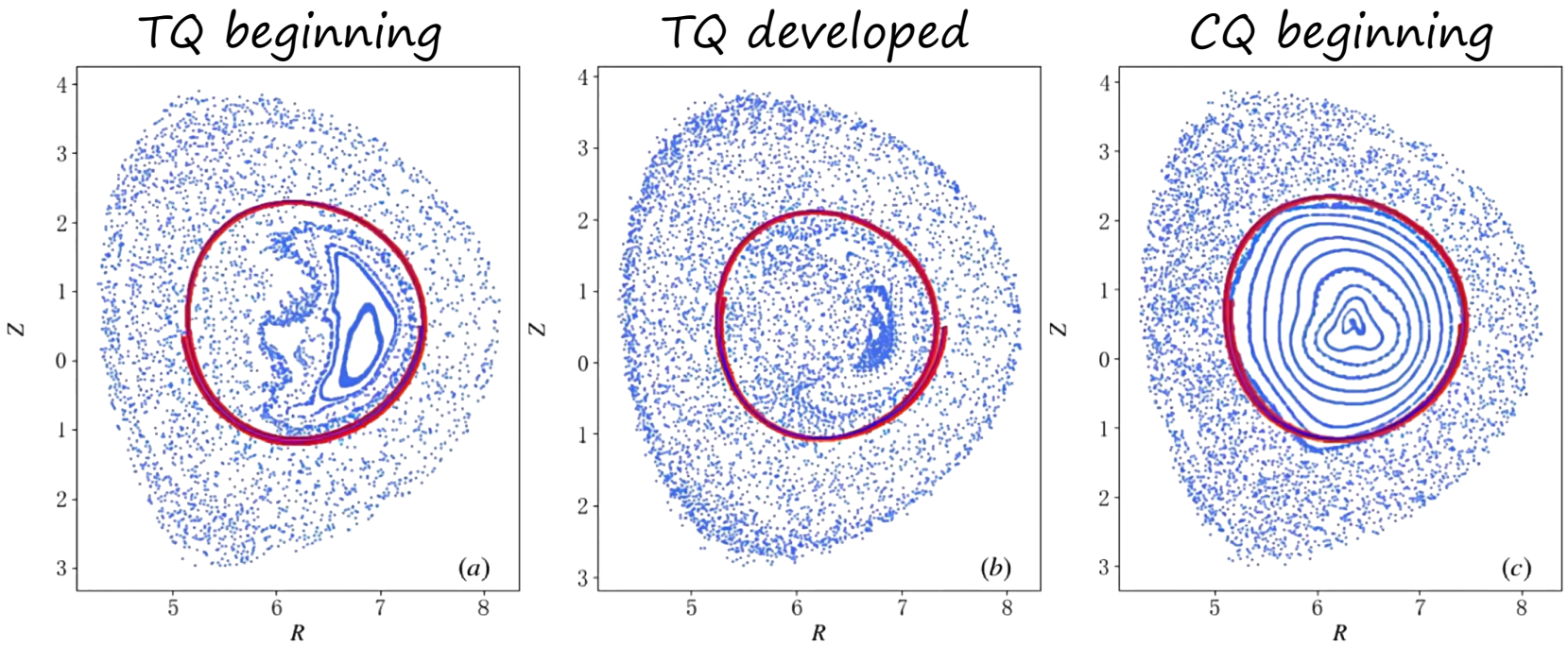

Magnetic field Poincaré-plot at $\phi = 0$ RZ-plane: (a) at the beginning of the thermal quench; (b) at the phase of the thermal quench; (c) at the beginning of the current quench.

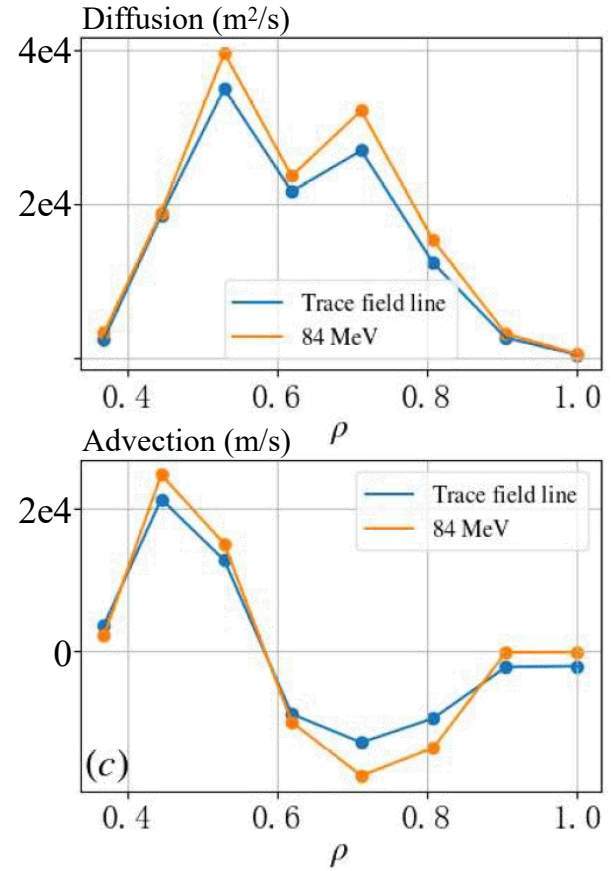

Diffusion and convection coefficient profiles for REs at CQ beginning.

- When orbit width ~ perturbation length, **FOW effect strongly alters transport**
- PTC has completed benchmark for **runaway electrons motion** for ITER

PTC Integrated into OMFIT Platform

Workflow

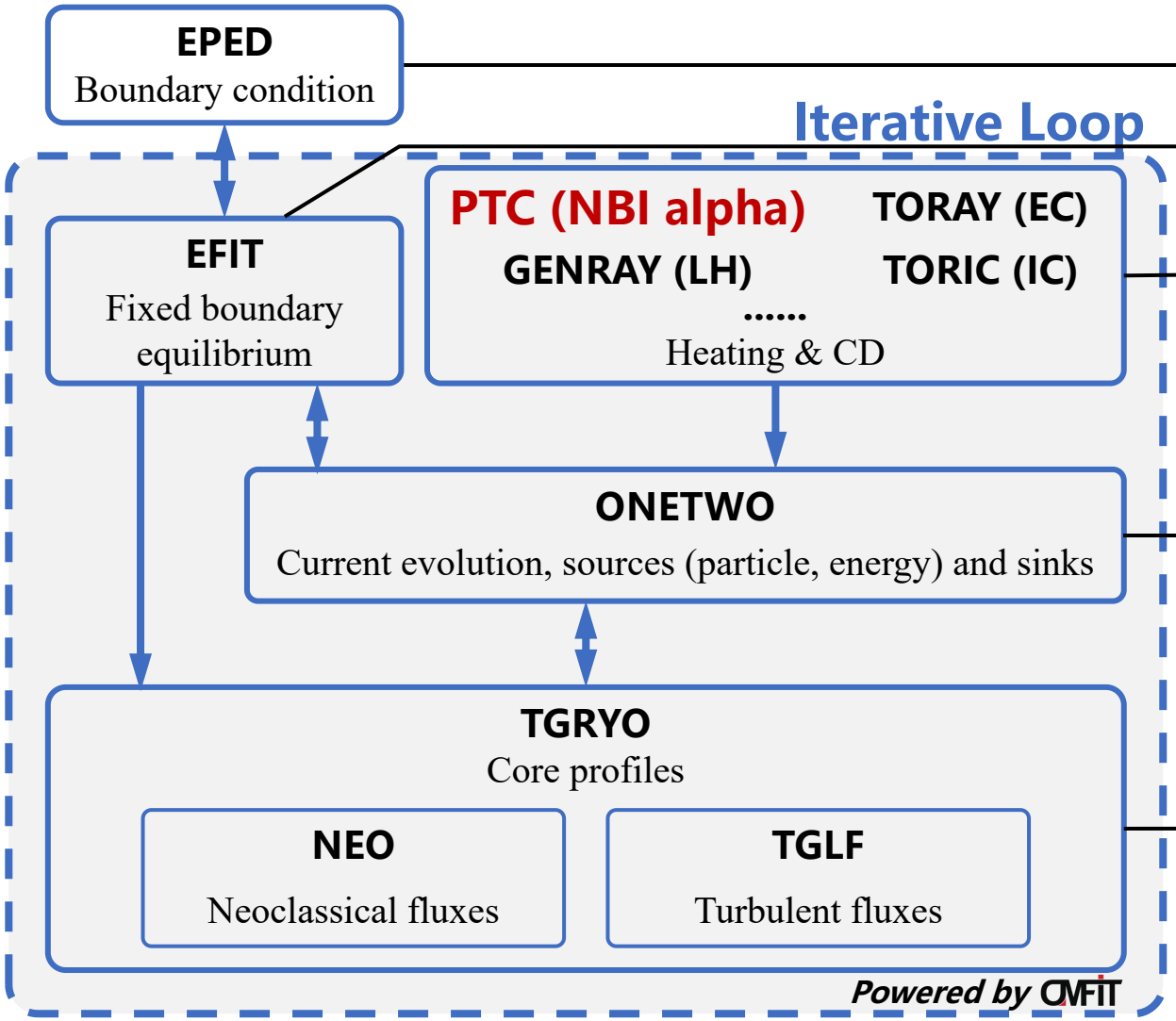

1. EPED is used to obtain the parameters of the pedestal region.
2. EFIT is employed to calculate the fixed-boundary equilibrium.
3. **PTC is applied to acquire the distribution of heating and current drive from NBI (Neutral Beam Injection) and fusion-produced alpha particles.**
4. ONETWO predicts the current profile, calculates the radiated power, and obtains the distribution of heating and current drive.
5. TGYRO predicts the core profile based on Flux-match (with TGLF and NEO used for core prediction).
6. Repeat steps 2 to 5 until a steady-state solution is obtained.

PTC Development Milestone

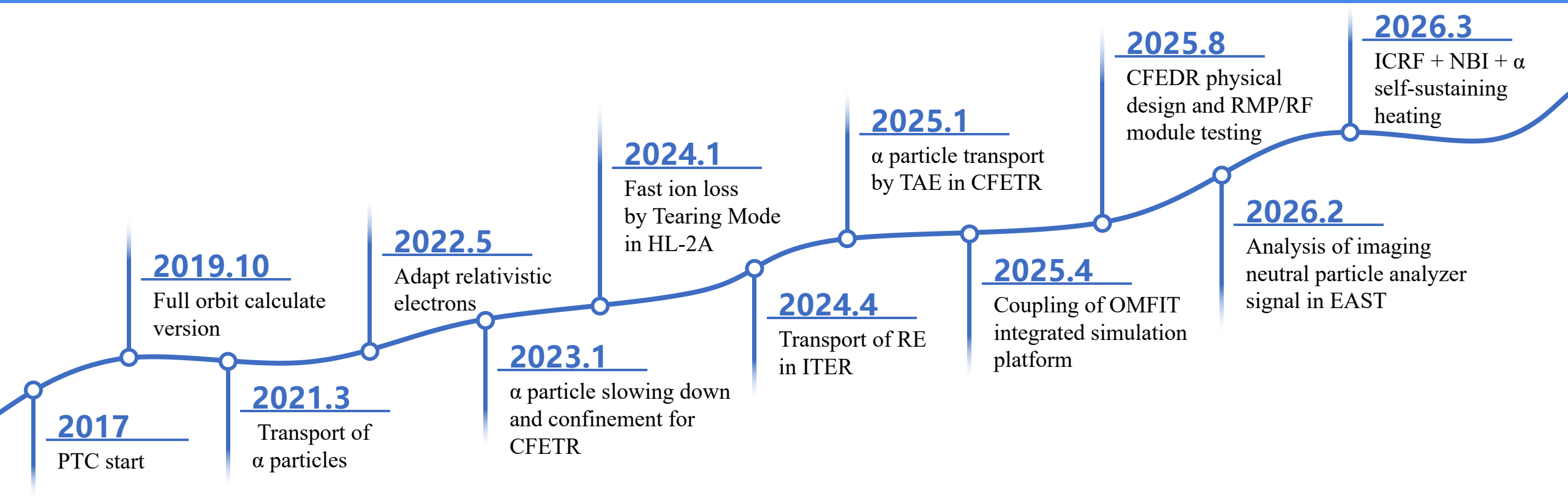

1. **F. Wang, *Chin. Phys. Lett.* 2021**
2. **S. Liu, *J. Plasma Phys.* 2022**
3. **X. Wu, *Acta Phys. Sin.* 2023**
4. **S. Liu, *Plasma Phys. Controlled Fusion* 2024**
5. **Y. Zhang, *Plasma Phys. Controlled Fusion* 2024**
6. **Z. Lin, *Plasma Sci. Technol.* 2024**
7. **R. Zhang, *Plasma Sci. Technol.* 2024**
8. **Y. Sun, *Nucl. Fusion* 2025**

Outline

1 Background

2 PTC Model: Fundamentals

3 **Applications**

1. Alpha particle transport with TAE

2. Analysis of IPNA signal for EAST

3. ICRH + NBI synergetic heating

4 Summary

Alpha Particle Transport with TAE

TAE instabilities in CFETR SS Scenario

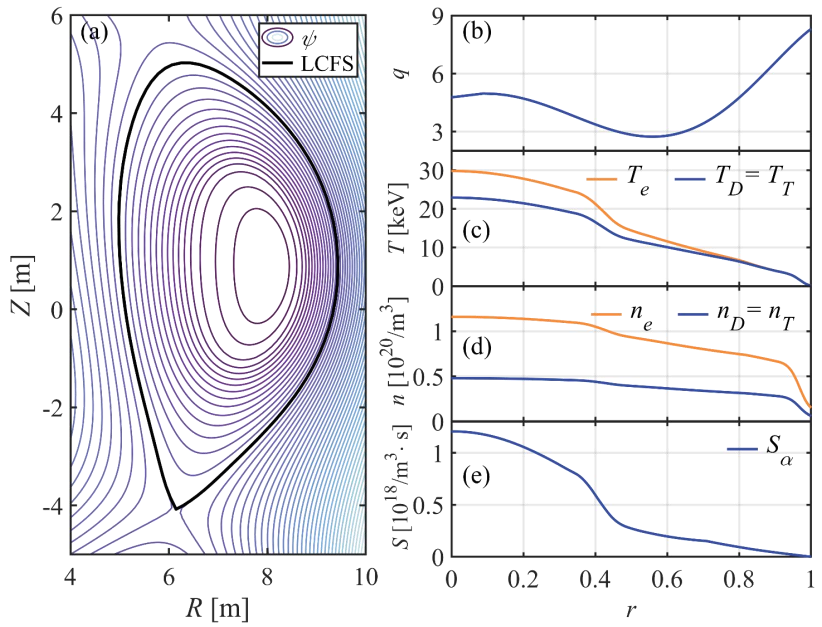

CFETR SS equilibrium and profiles.

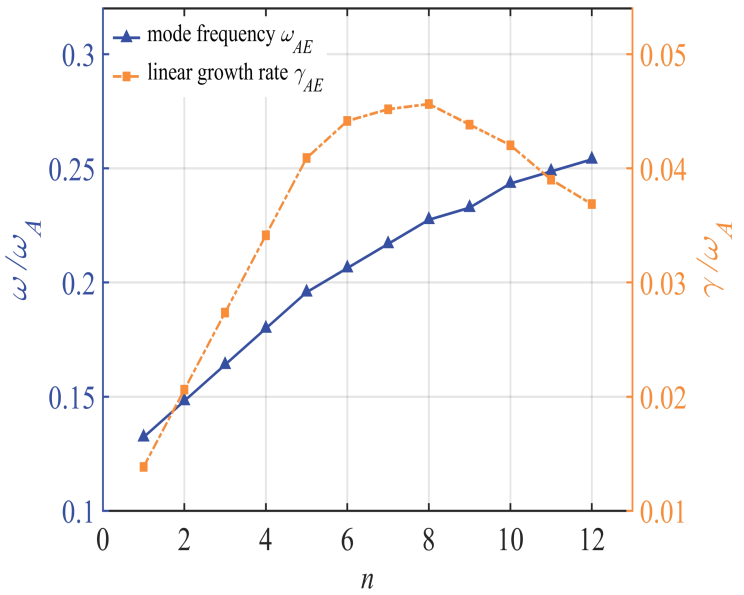

Mode frequency and linear growth rate of different n TAE.

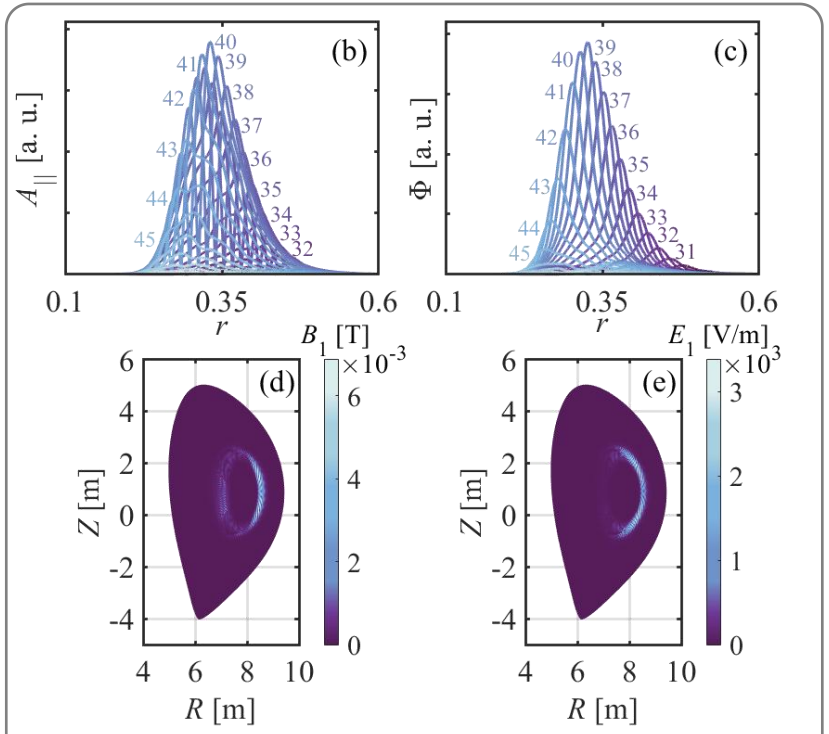

$n = 10$ TAE mode radial structure and poloidal distribution.

In CFETR, **the most unstable α-driven TAEs have higher n ($n = 7\sim10$)** than in existing tokamaks **($n = 1\sim4$)** [1], implying more complex transport feature of α particles

[1] Zhen-Zhen Ren *et al, Nucl. Fusion,* 2024

Alpha Particle Transport with TAE

α particles transport in TAE linear phase for CFETR

Nucl. Fusion 2026

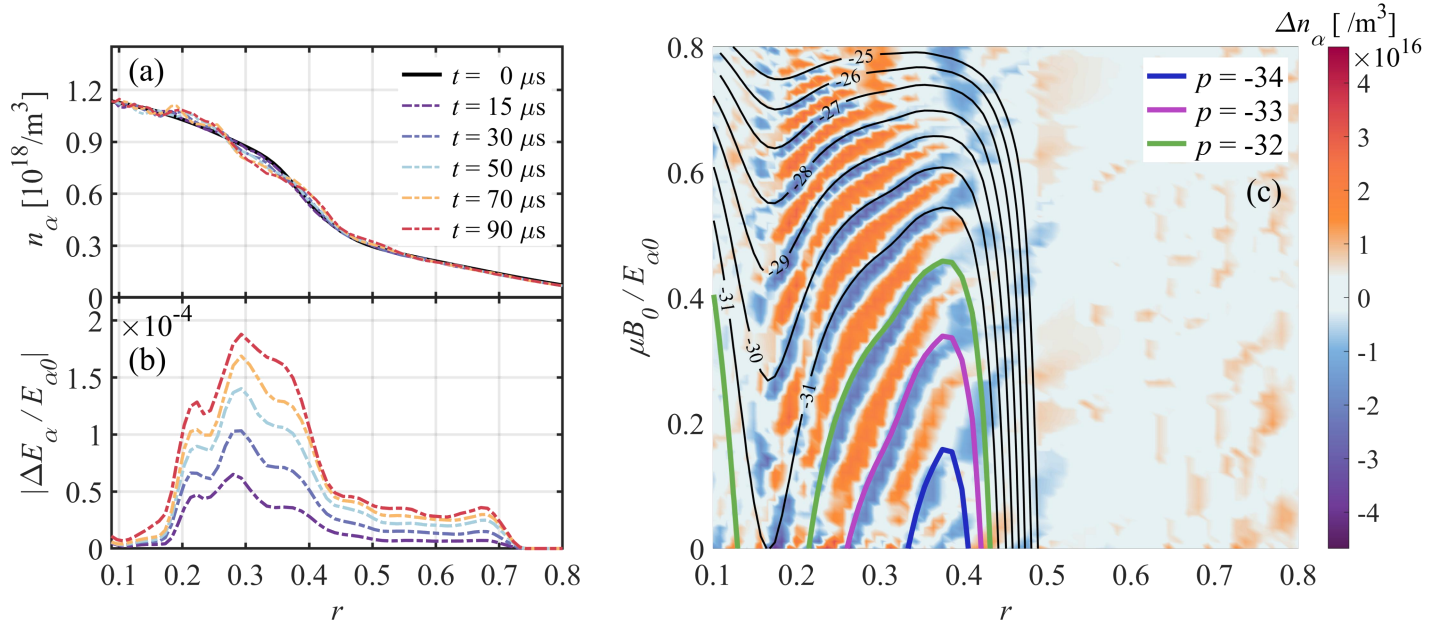

Evolution of (a) density profiles and (b) energy variation profiles of α particles. (c) Density variation distribution in the $r-\mu$ phase space at t =50μ s.

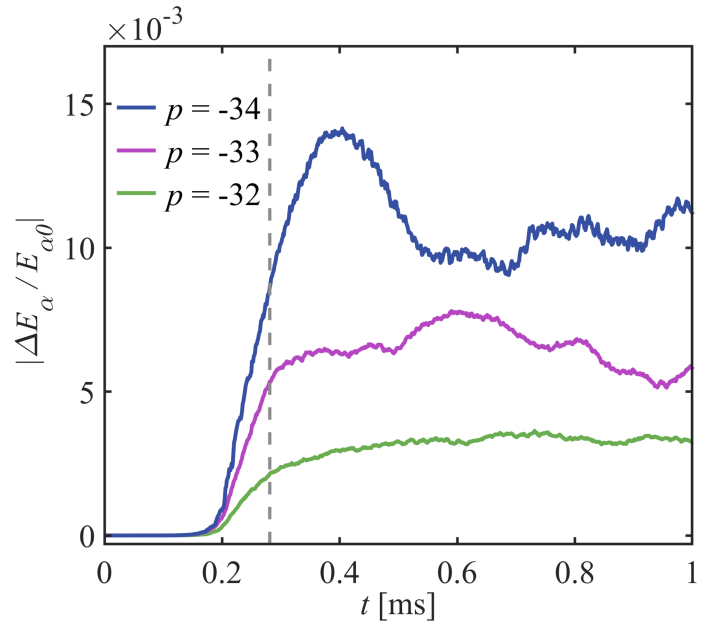

Temporal evolution of energy variation for different resonant particles.

- Resonant α particles move to core & boundary with resonance: $\omega_{AE} = n\omega_\phi + p\omega_\theta$
- Over time, **$|\Delta E|$ and $|\Delta n|$ increase**, and **TAE has a larger radial influence region**
- The strongest resonance relations for $n = 10$ TAE are: p =−34 ~ −32

Alpha Particle Transport with TAE

Evolution of α particles in the nonlinear phase of weak TAE

Nucl. Fusion 2026

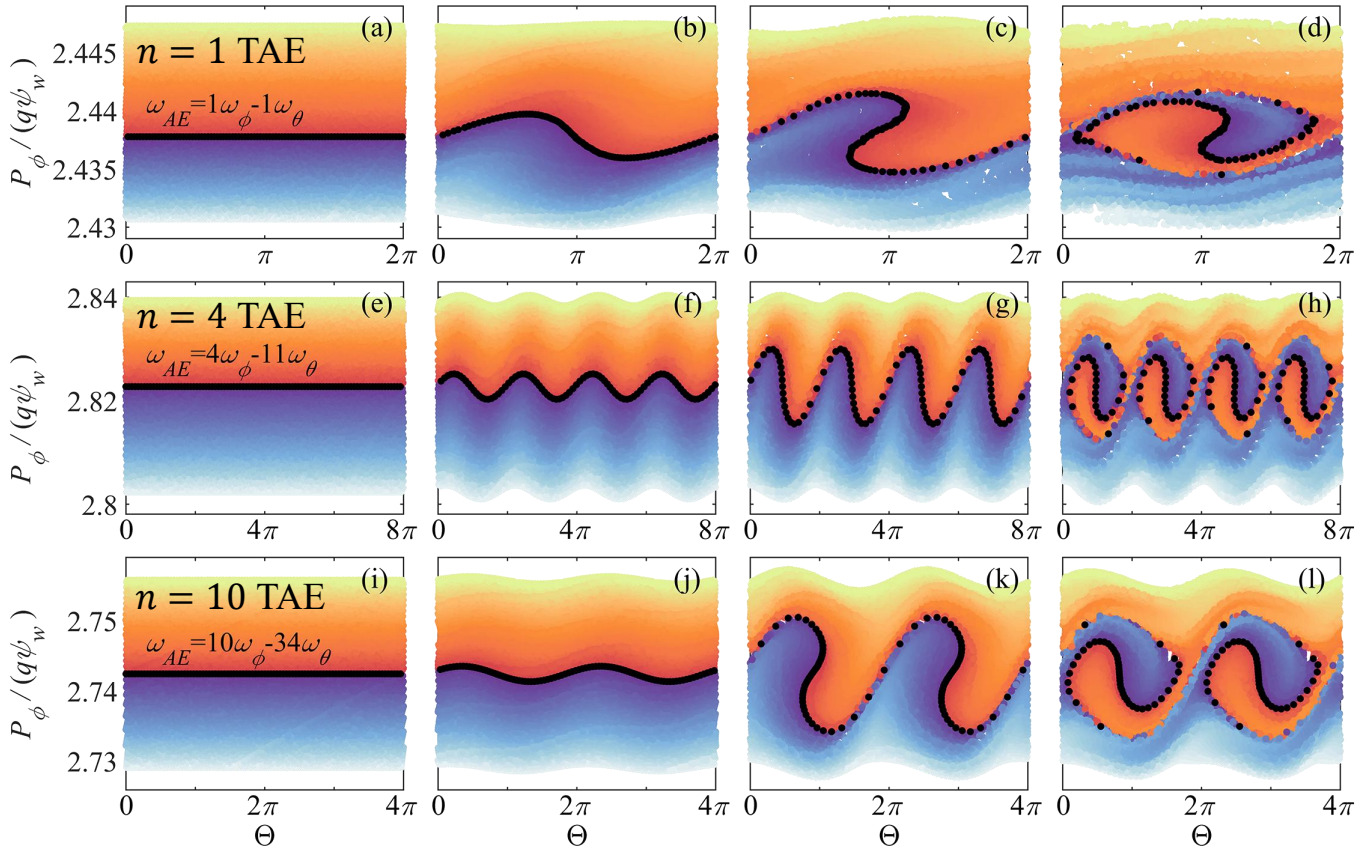

Poincaré plots of α particles near resonance in the $\Theta - P_\phi$ phase space under TAE perturbations with $n = 1,\ 4,\ 10$.

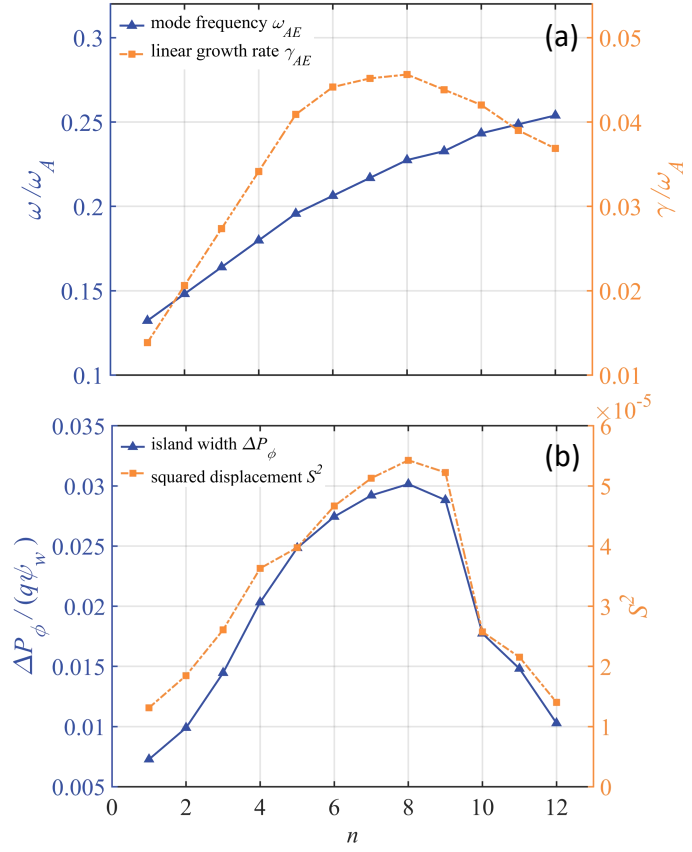

Comparison of island width and displacement variation under different n -TAE modes.

■ $n = 10$ TAE has the most significant impact on the radial transport of α particles

Alpha Particle Transport with TAE

Evolution of α particles in the nonlinear phase of strong TAE

Nucl. Fusion 2026

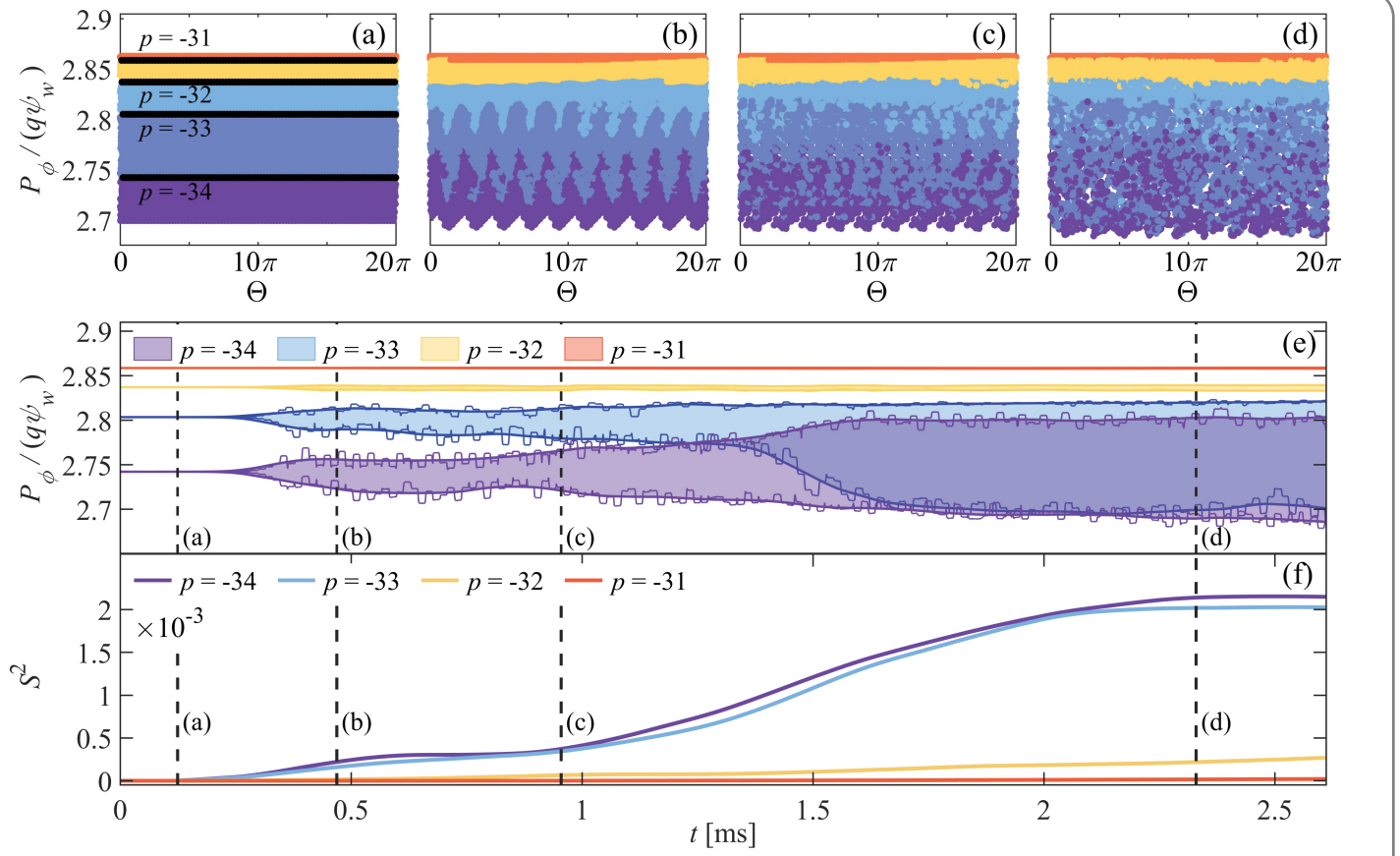

Under strong $n = 10$ TAE: (a)-(d) phase space distributions of resonant α particles in $\Theta - P_\phi$; (e) radial range of P_ϕ; (f) radial displacement S^2.

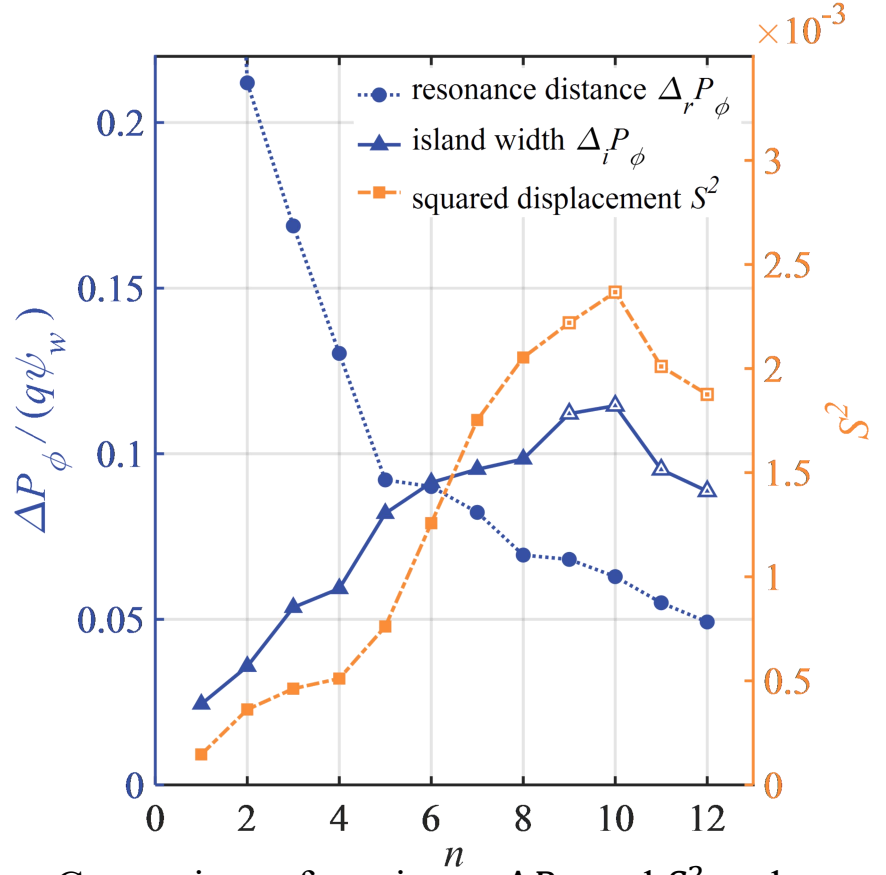

Comparison of maximum ΔP_ϕ and S^2 under different n -TAE modes.

■ **Resonance overlap** significantly enhances the radial transport of α particles

Outline

1 Background

2 PTC Model: Fundamentals

3 **Applications**

1. Alpha particle transport with TAE
2. **Analysis of IPNA signal for EAST**
3. ICRH + NBI synergetic heating

4 Summary

Analysis of IPNA Signal for EAST

Imaging Neutral Particle Analyzer (INPA): Get energy, pitch, location of fast ions

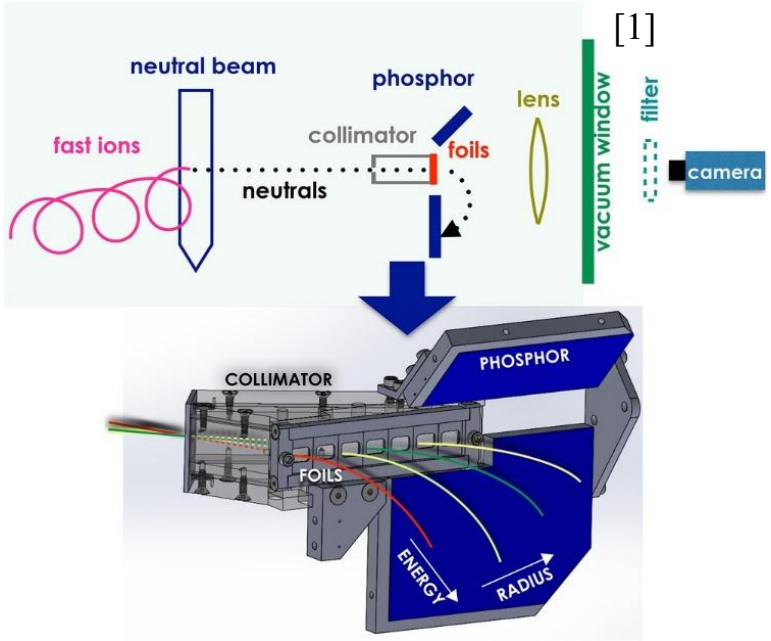

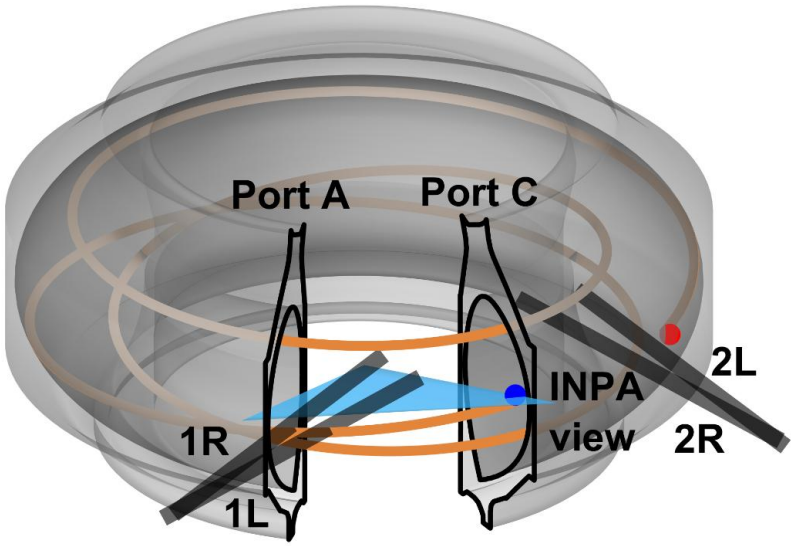

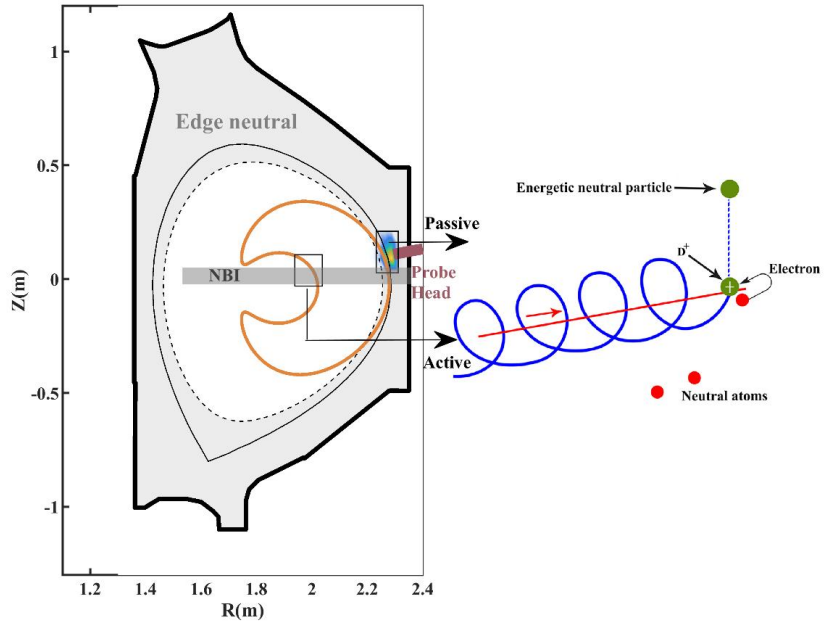

- **INPA enables inference of N_i & T_i, fast ion transport, and wave-particle interactions**
- **Active/ Passive signal : Charge exchange btw fast ion and beam/edge neutrals**

[1] X.D. Du. *Nucl. Fusion,* 2018

Analysis of IPNA Signal for EAST

Double-peaked feature: passive signals in pitch angle for EAST

Nucl. Fusion 2026

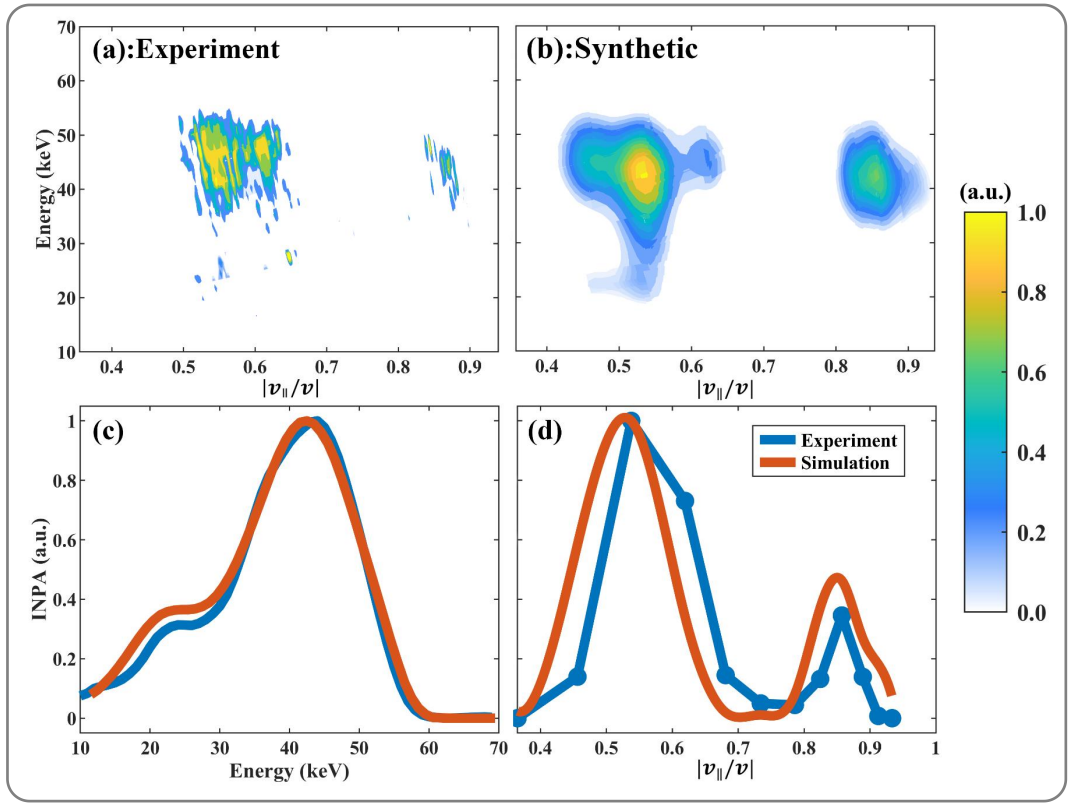

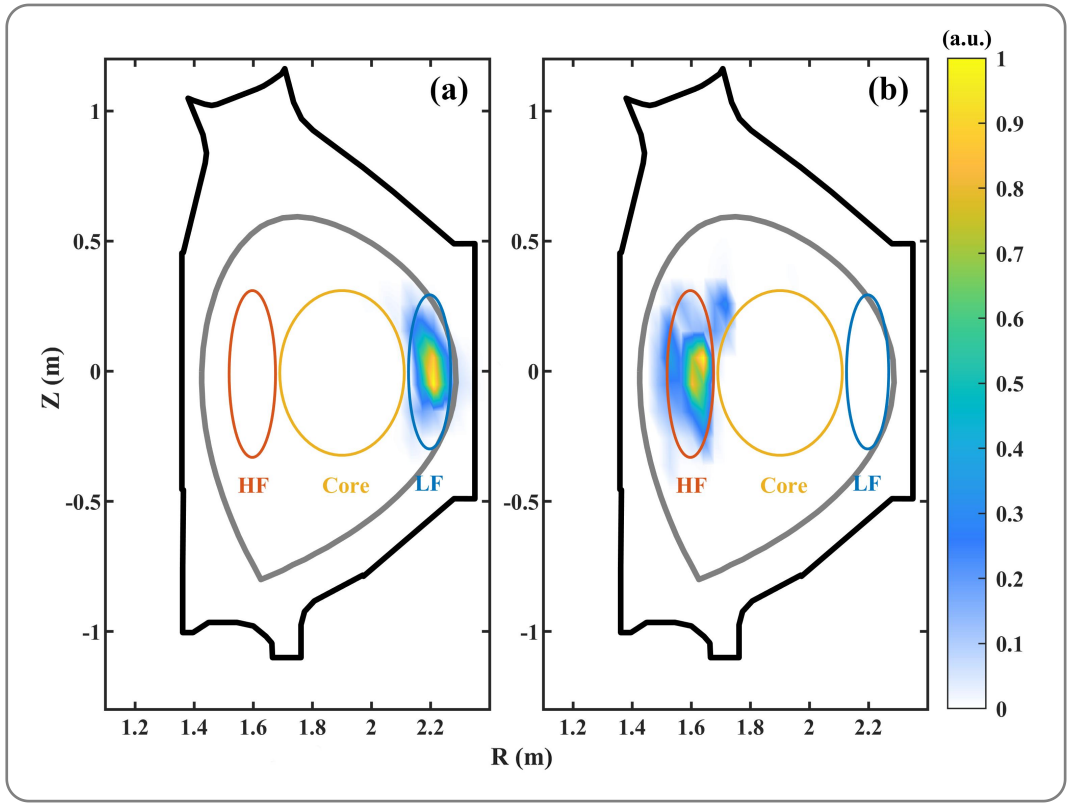

- A good agreement is obtained between PTC-synthetic and experimental images
- Double-peaked is from fast ions initially deposited on **low-** and **high-field side**

Analysis of IPNA Signal for EAST

Peak ratio is related with n_e and β_N

INPA peak ratio = higher peak / lower peak

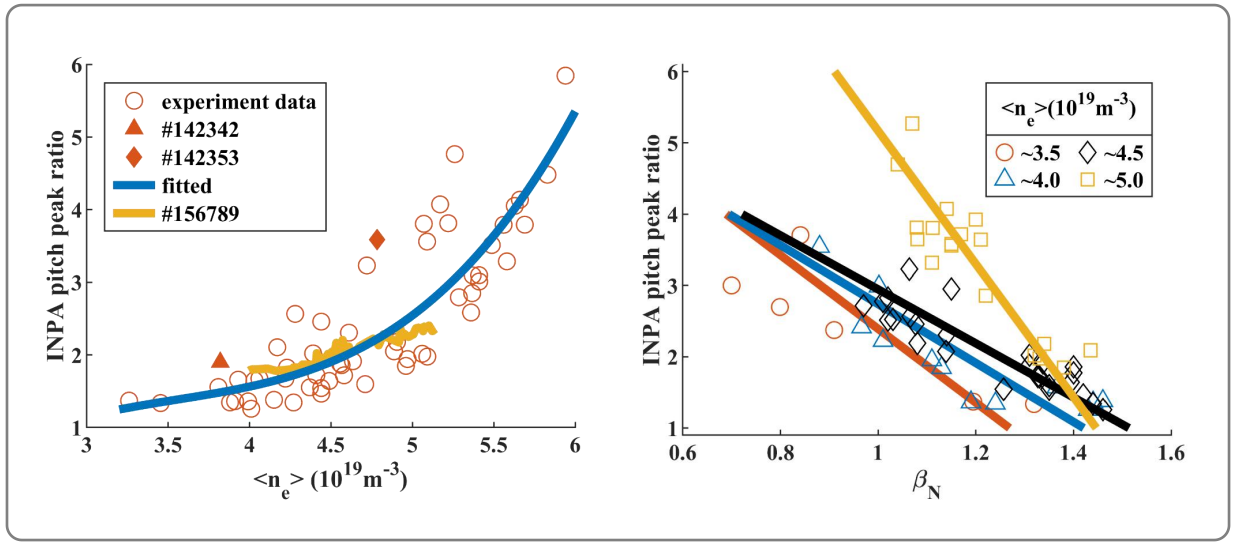

Nucl. Fusion 2026

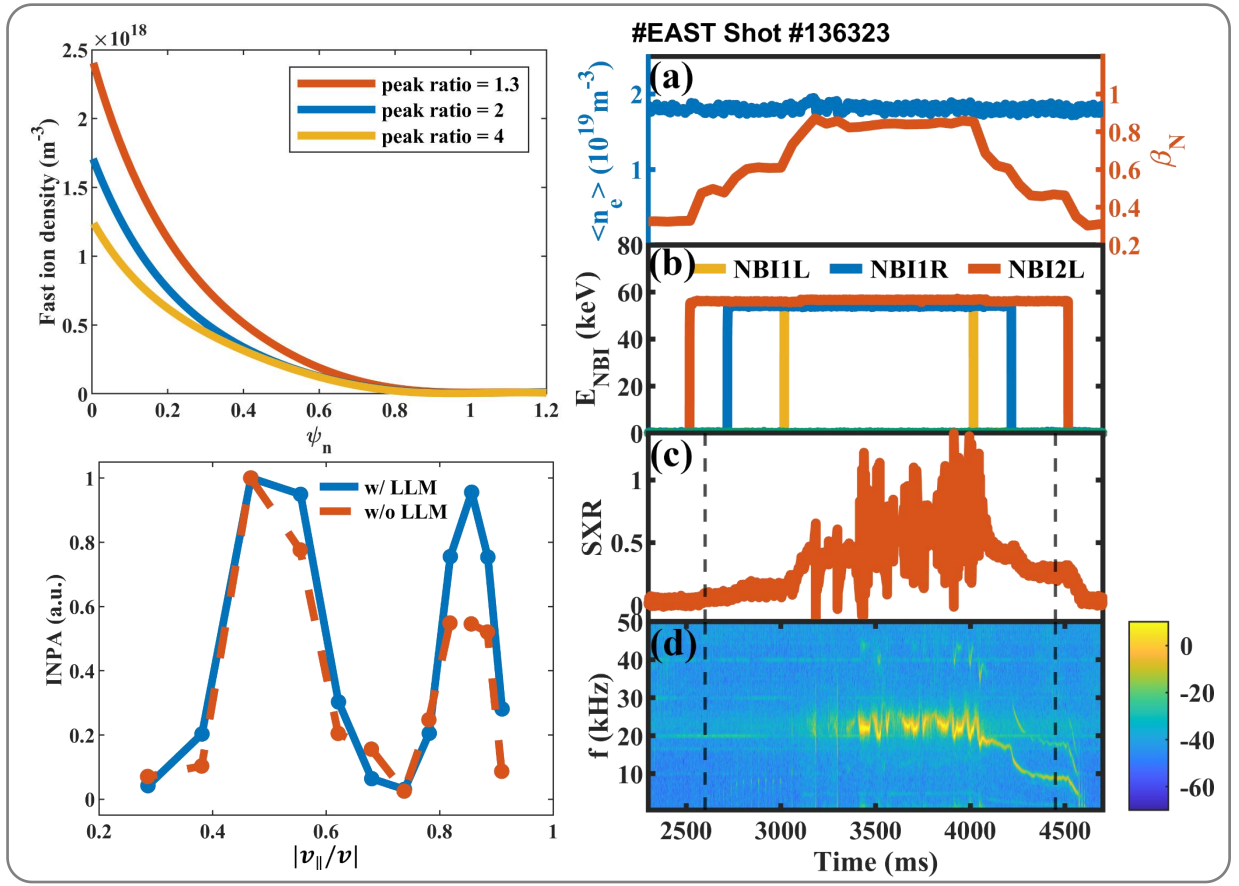

- Peak ratio increases with $\uparrow n_e$ and $\downarrow \beta_N$, suggesting an indicator of EP confinement
- Lower peak ratio corresponds to a steeper fast ion pre gradient, triggering LLM

Analysis of IPNA Signal for EAST

Double-peaked feature after SMBI for EAST

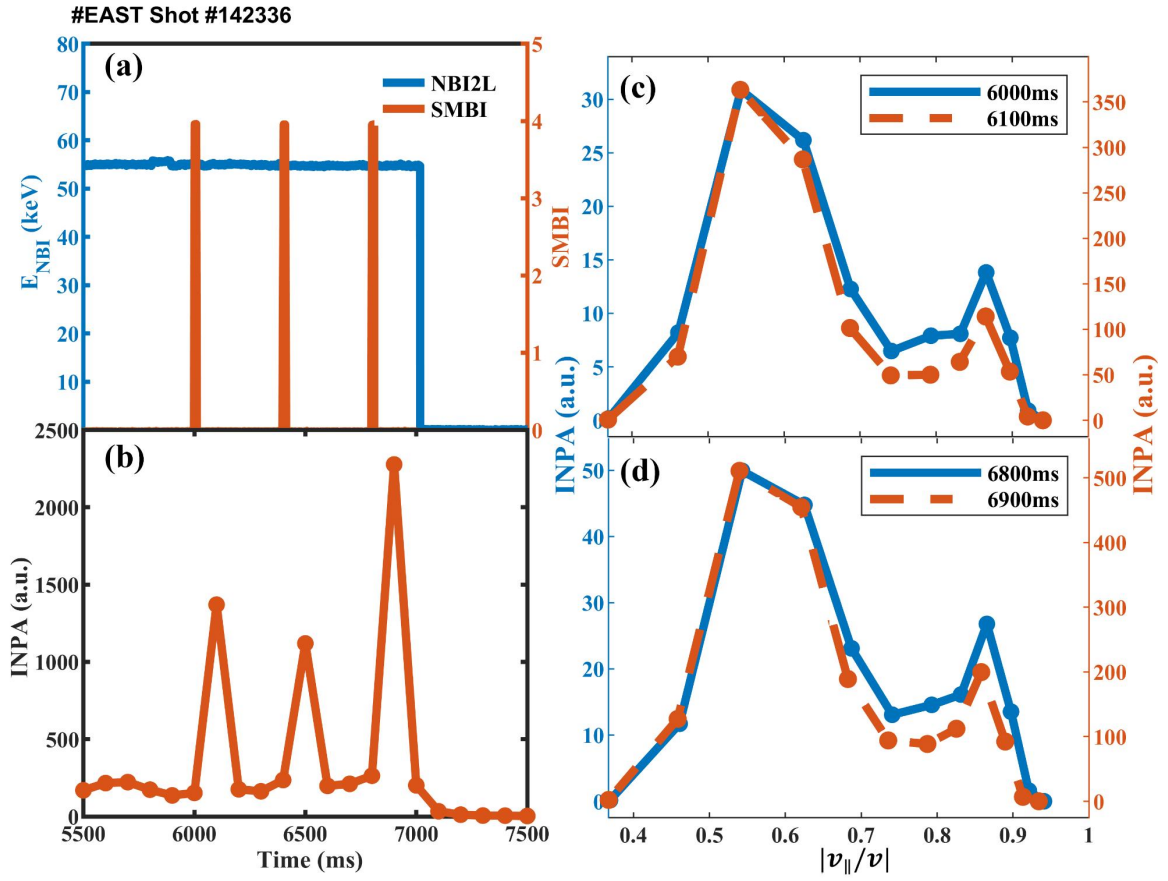

Variation of double-peaked distribution after SMBI injection.

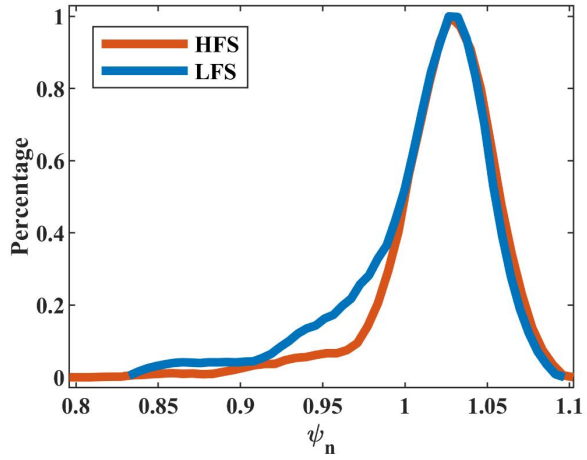

The distribution of fast ion contributing to higher peak (blue) and lower peak (red).

- After SMBI, signal intensity increases **an order**
- Proportion of low pitch peak is decreased,
- Still, double-peak is notably **maintained**

Nucl. Fusion 2026

Outline

1 Background

2 PTC Model: Fundamentals

3 **Applications**

1. Alpha particle transport with TAE
2. Analysis of IPNA signal for EAST
3. **ICRH + NBI synergetic heating**

4 Summary

ICRH + NBI Synergetic Heating

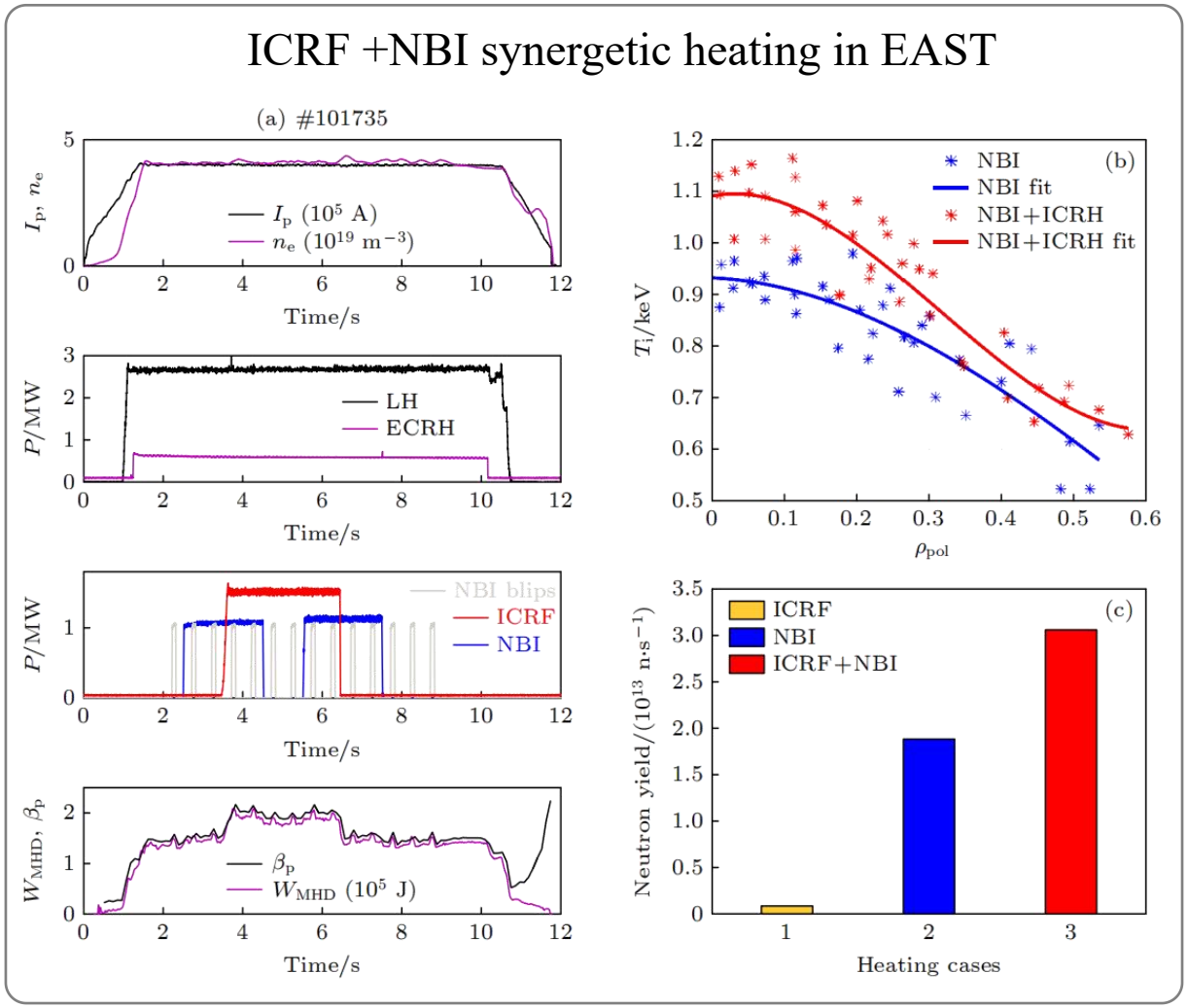

ICRF Heating in Magnetic Confinement Fusion

- One of effective heating methods for fusion plasmas
- Transfers energy to ions via wave-particle resonance
- Critical for present (EAST, JET) and future (ITER, CFEDR) fusion devices

ICRF-NBI Synergy

- Fast ion energy and deposition efficiency are enhanced
- Experimental results (EAST): 36% β_p increase, 35% plasma stored energy increase, 20% core ion temp increase, 100% neutron yield increase

Motivation

- Accurate self-consistent modeling of ICRF + NBI synergy heating
- PTC extended to include ICRF + NBI heating

ICRH + NBI Synergetic Heating

RF heating module in PTC

Phys. Plasmas 2026

■ **Full orbit simulation** (nonlinear):

Solve 6D Lorentz equation with RF fields as perturbations; high accuracy but computationally expensive.

$$m d_t \boldsymbol{v}(\boldsymbol{x},t) = q\left[\boldsymbol{v}\times\left(\boldsymbol{B}_0(\boldsymbol{x})+\tilde{\boldsymbol{B}}(\boldsymbol{x},t)\right)+\tilde{\boldsymbol{E}}(\boldsymbol{x},t)\right]. \qquad \tilde{\boldsymbol{E}}(\boldsymbol{x},t)=\tilde{\boldsymbol{E}}_{n,\omega}(R,Z)\exp\left(in\phi-i\omega t\right).$$

■ **Guiding center + quasi-linear operator** (practical):

Orbit-averaged Fokker-Planck equation; dominant approach for this work.

new set invariants introduced by Eriksson [2005]: $$I_\perp=\frac{m\omega}{n_1 q}\mu, \quad I_\parallel=\mathscr{E}-I_\perp, \quad I_\phi=p_\phi-\frac{n_3}{\omega}\mathscr{E}$$

Orbit averaged kinetic equation: $$\frac{\partial f_0}{\partial t}=\frac{1}{\tau_b}\frac{\partial}{\partial I_\perp}\left(\tau_b\omega^2 D_{0s}\frac{\partial f_0}{\partial I_\perp}\right) \qquad D_{0s}=\frac{1}{2\tau_b}\frac{q^2}{\omega^2}v_\perp^2 s_n^2\tau_{\text{eff}}^2$$

$$\Delta I_\perp=\frac{\partial}{\partial I_\perp}\left(\tau_b\omega^2 D_{0s}\right)\frac{\Delta t}{\tau_b}+R\sqrt{2\tau_b\omega^2 D_{0s}\frac{\Delta t}{\tau_b}} \qquad \Delta v_\perp^2=\left(4\beta^2\frac{\partial}{\partial v_\perp^2}+2\gamma\beta^2\frac{\partial}{\partial v_\parallel}\right)d_{0s}\frac{\Delta t}{\tau_b}+R\sqrt{2\frac{\Delta t}{\tau_b}\sqrt{4\beta^2 d_{0s}}}$$

$$\Delta v_\parallel=\left(2\gamma\beta^2\frac{\partial}{\partial v_\perp^2}+\gamma^2\beta^2\frac{\partial}{\partial v_\parallel}\right)d_{0s}\frac{\Delta t}{\tau_b}+R\sqrt{2\frac{\Delta t}{\tau_b}\sqrt{\gamma^2\beta^2 d_{0s}}}$$

ICRH + NBI Synergetic Heating

Workflow for both ICRF and NBI heating

Phys. Plasmas 2026

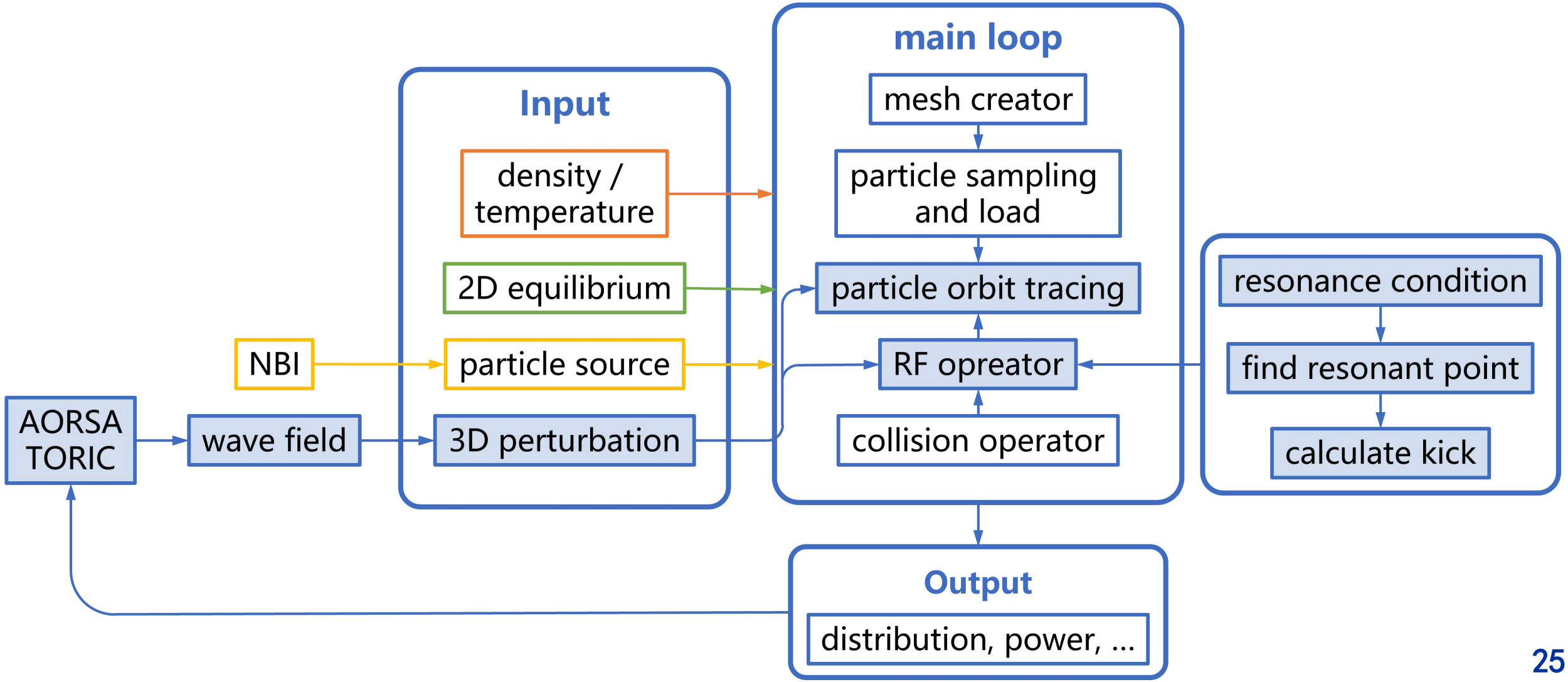

ICRH + NBI Synergetic Heating

Comparison with CQL3D

Phys. Plasmas 2026

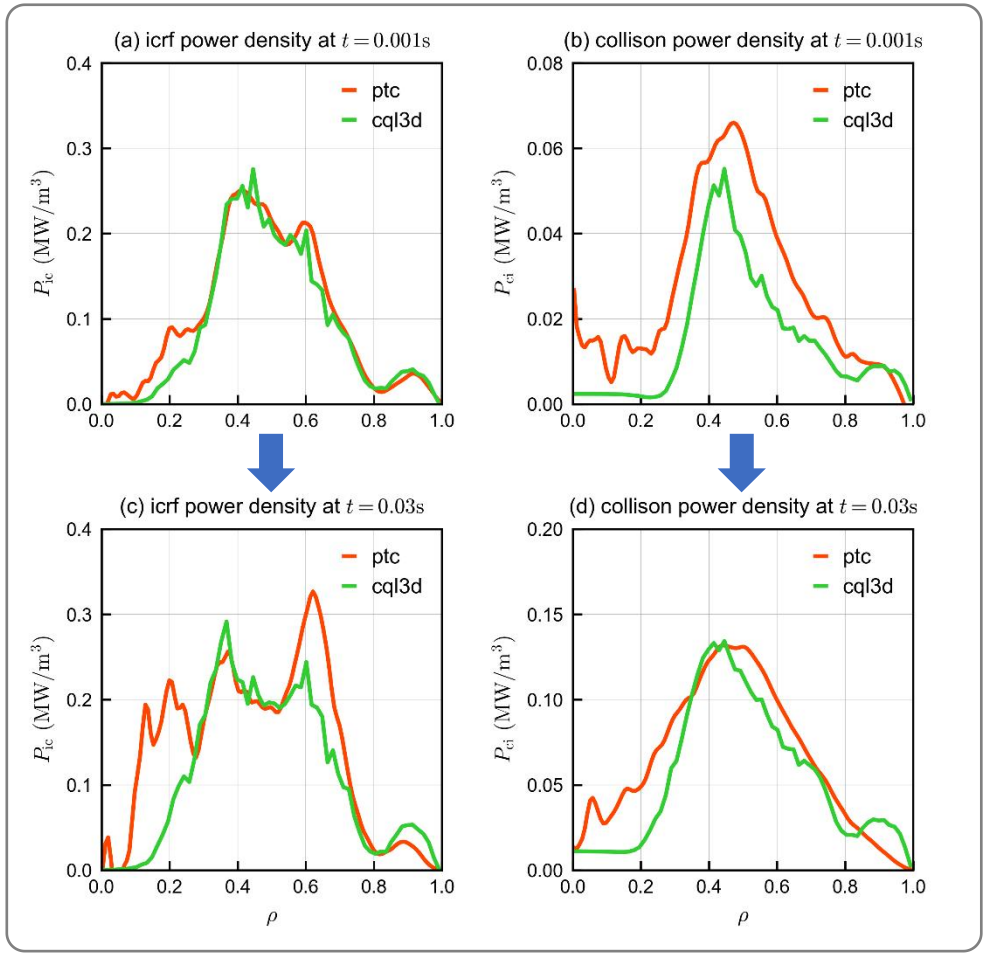

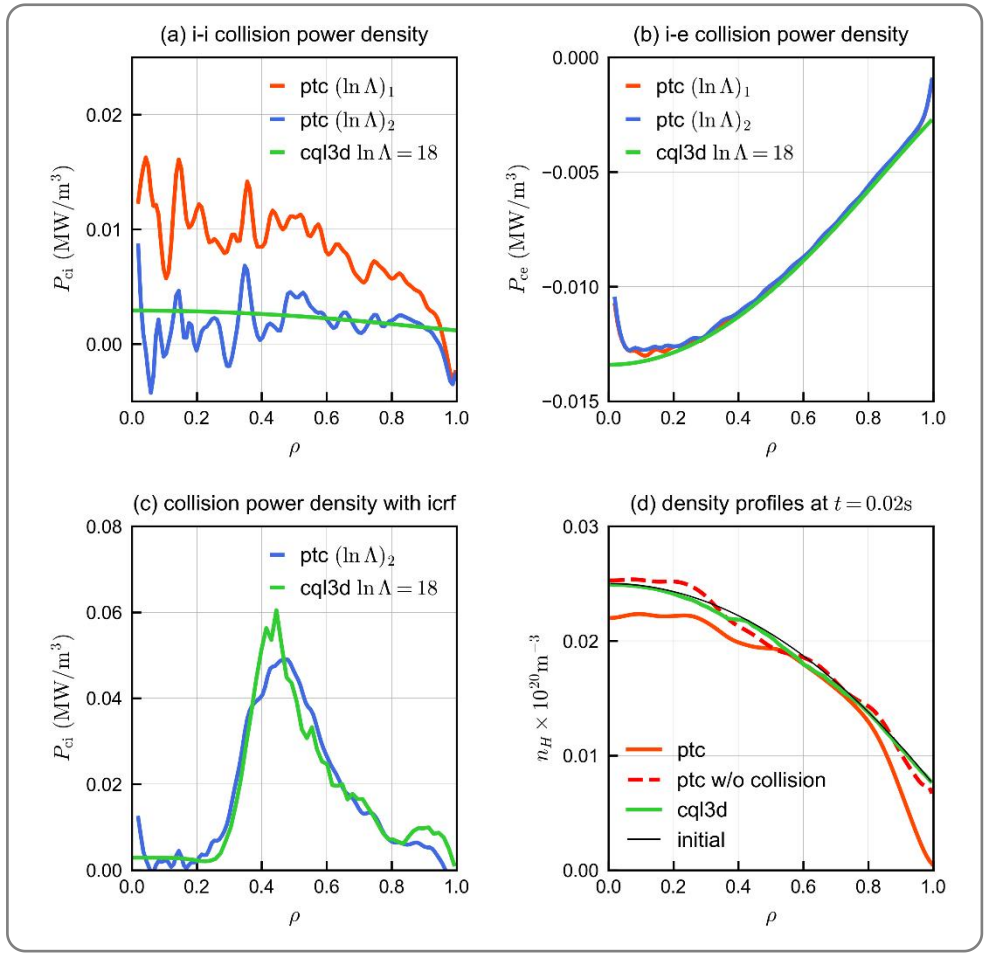

- Zero orbit width in CQL3D gives no density evolution
- **FOW effect** in PTC broadens power deposition region
- PTC agrees with CQL3D for fixed $\ln\Lambda$ cases
- but PTC uses a **more complete collision description**

ICRH + NBI Synergetic Heating

Numerical Results

Phys. Plasmas 2026

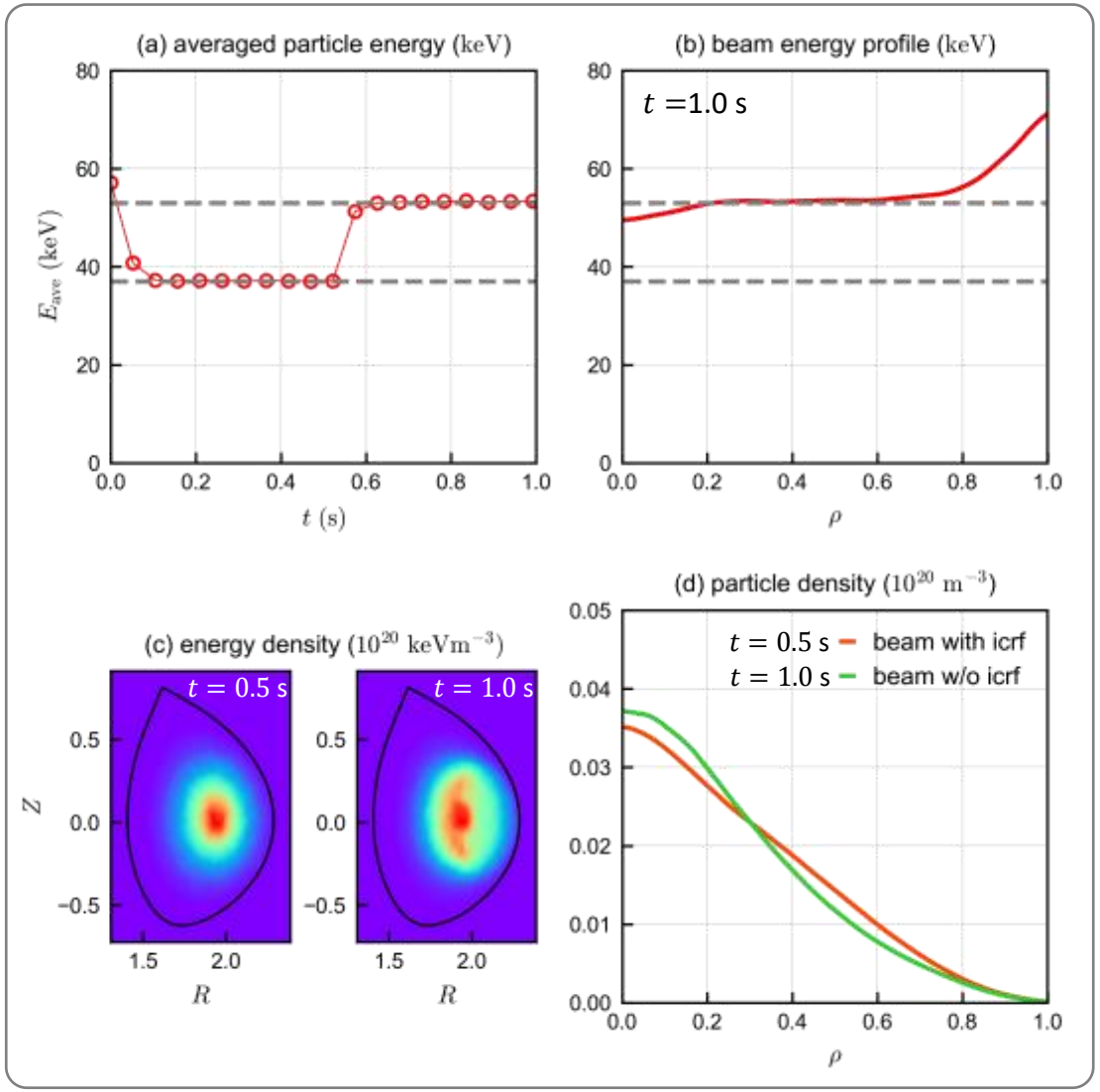

NBI preheating process

- Beam ions slow down from ~60 keV to 37 keV (~0.1 s) via collisions
- Beam ion density peaks at magnetic axis (8% of total ion density in core)
- NBI-modified thermal/beam ion density profiles for subsequent ICRF heating

ICRF heating results

- ICRF acceleration gives a higher-energy-tail of beam ions
- ICRF induce more asymmetric energy density distribution

Outline

1 Background

2 PTC Model: Fundamentals

3 Applications

4 **Summary**

Summary

PTC Core Capability Development

Evolved with new capabilities like guiding center tracking, collision operators, and interfaces with external solvers, becoming a versatile tool for standalone and integrated modeling.

High-n TAE Effects

In CFETR-like large tokamak fusion reactor plasma, **high-n TAEs cause greater α particle transport**. Furthermore, resonance overlap occurs more readily under the high-n TAEs, which further enhances the resonant α particle transport.

INPA Signal Validation

PTC simulation reveals that the bimodal pitch distribution of INPA passive signals originates from fast ions initially deposited on the low- and high-field sides, demonstrating **the potential of passive signals for inferring fast ion transport**.

ICRF & NBI Synergy

The PTC extension for ICRF heating showing good agreement with AORSA and CQL3D. And ICRF-NBI synergy simulations demonstrate that ICRF significantly boosts beam ion energy, reaching convergence within 2–3 iterations.

Thanks for your attention!

Develop Particle-Orbit-Tracking Model for Tokamak Burning Plasmas

Zheng-Xiong Wang

Dalian University of Technology, Dalian, China